Artificial Composite Materials Consisting of Nonlinearly Loaded Electrically Small Antennas: Operational-Amplifier-Based Circuits with Applications to Smart Skins

Fabrice Auzanneau and Richard W. Ziolkowski, *Fellow, IEEE*

***Abstract*—Several new artificial nonlinear composite materials are introduced in this paper. They consist of electric molecules constructed with nonlinearly loaded electrically small dipole antennas. Their behaviors are studied with an augmented finite-difference time-domain (FDTD) simulator. The loads are based upon the use of multiple diodes and ideal operational amplifiers. The resulting composite materials are shown to have nonlinear electromagnetic properties including the ability to create any desired set of harmonics and subharmonics from an input wave having a single fixed frequency. Curve shaping circuits are introduced, simulated, and used to design materials that produce output signals of specified forms. Because the operating points of these curve shapers are adjustable, they could be modified in real time. The resulting smart materials could be designed in the microwave region to produce any specified response to a recognized input signal.**

***Index Terms*— Electromagnetic propagation in nonlinear media, electromagnetic scattering by nonlinear media, nonhomogeneous media.**

I. Introduction

THERE are many potential applications of artificial dielectric and magnetic materials to microwave wave engineering. Engineers in their unending quest to improve device and system performances are beginning to utilize a variety of complex materials to increase the degrees of freedom available to them in the design and fabrication processes. Artificial materials are a potent source for designable and controllable electric and magnetic properties. Artificial chiral materials [1]–[3] have been studied extensively in recent years in this context in an attempt to realize more efficient radar absorbing coatings. Metallic helixes embedded in dielectric substrates have led to bianisotropic materials with interesting electric and magnetic properties.

We have introduced elsewhere [4]–[8] the concept of constructing electric and magnetic artificial materials using "molecules," the term we introduce to denote the constituent electrically small antennas connected to specified passive linear electronic loads. By varying the loads, we have demonstrated that the properties of these materials can be designed for a variety of applications. Traditional material behaviors, the Debye and Lorentz models, as well as their generalizations to include more inclusive polarization and magnetization excitations, the time-derivative Debye, time-derivative Lorentz, two time-derivative Lorentz, etc., models, have been realized in this manner. Numerical simulations have demonstrated their efficacy individually as electrically or magnetically lossy dispersive materials as well as in matched combinations to form nonreflective absorbers.

With the increase of activity in utilizing active elements in many RF systems [9]–[17], we have been led to the idea of incorporating nonlinear components into the loads which form these artificial molecules. The degrees of freedom in the variations in the behaviors of the individual molecules increase dramatically. The use of passive nonlinear loads based upon diodes has been considered in detail elsewhere [18] and is extended here by introducing loads consisting of multiple diodes to achieve specific frequency and time-domain outputs. Using multiple diodes, one can encode different signal information on the positive and negative portions of the input waveform.

We begin Section II with a brief summary of our concepts of the electric molecules; i.e., the loaded electrically small dipole antennas and their modelizations. We then use the passive multiple diode configuration to provide a rudimentary, but interesting case with which we explain the procedure for developing the equation system which represents the augmented finite-difference time-domain (FDTD) simulator. Furthermore, this passive nonlinear load example nicely demonstrates the fact that the scattered field response can mimic the load response. Since all of the circuit behavior predictions from the augmented FDTD simulator are first checked against the corresponding SPICE calculations, this example also illustrates how we tested the validity of the augmented FDTD simulation results. Because nonlinear problems in general can only be validated against experimental or other code results, these comparisons are a crucial aspect of our simulation process. We selected the numerical FDTD approach rather than a more analytical Volterra series technique for our simulations to

Manuscript received August 22, 1997; revised March 27, 1999. This work was supported in part by the Office of Naval Research under Grant N0014-95-1-0636 and by the Air Force Office of Scientific Research, Air Force Material Command, USAF under Grant F49620-96-1-0039.

F. Auzanneau is with CEA CESTA, 33114 Le Barp, France.

R. W. Ziolkowski is with the Department of Electrical and Computer Engineering, The University of Arizona, Tucson, AZ 85721 USA.

Publisher Item Identifier S 0018-926X(99)07963-6.

take advantage of the flexibility of the FDTD method. We were interested in large amplitude, large frequency bandwidth results which were readily accessible through the augmented FDTD simulator.

In Section III, we further extend the classes of nonlinear loads through the use of active nonlinear devices based upon the introduction of operational amplifiers (op amps) into the load circuits. The op amp circuits are introduced and our analysis is extended to the resulting nonlinearly loaded antennas to achieve an accurate assessment of their behaviors. The necessary augmentations to the FDTD simulator created for these investigations are emphasized. We demonstrate the utility of the approach using an op amp differentiator molecule. We show that a composite active material consisting of these molecules will produce multiple and even half (i.e., sub) harmonics when it is driven with an incident narrow bandwidth pulsed plane wave.

We further extend in Section IV the classes of nonlinear loads developed from the op-amp-based load circuits to include negative impedance transformers and phase shifters. A composite active material, which has a small refractive index and an adjustable loss tangent at any frequency, is designed and its behavior is characterized. We then introduce the curve shaping molecules in Section V. Utilizing curve shaping circuits obtained with more complex op-amp-based loads, we design molecules that lead to active materials that, given a specified input signal, respond with a specific predetermined output signal. The design of the output waveform is discussed and scattered field results are obtained to illustrate the potential merits of such a composite material. Because the operating points of these curve shapers are adjustable, we emphasize the fact that these "smart molecules" could be modified in real time. The resulting active smart molecule material could have a number of potentially interesting applications. We finalize our discussions and give our conclusions in Section VI.

We recognize that the ability to fabricate the types of molecules we are suggesting is limited today to the lower microwave region, e.g., 500 MHz to 10 GHz. This is due to the frequency response of the components (e.g., the op amps). Nonetheless, we feel that with the anticipated improvements in fabrication technologies and the desires for components with ever increasing frequency responses, the nonlinear molecules under consideration here may be extended to the higher microwave and even to the millimeter regime in the future.

II. Nonlinearly Loaded Antennas

We consider here electrically small loaded dipole antennas, as shown in Fig. 1. The dipole antenna has the half-length l_0 and wire diameter a_d. We denote the dipole antenna connected to its load (electronic circuit) as an "electric molecule." In the case of a linear load, we can derive [4]–[8] the electric susceptibility χ_e of the electric molecule by considering the input impedance of the antenna Z_{in} and the impedance of the load Z_L. We have shown that

$$\chi_e = \frac{K_e}{-j\omega(Z_{\text{in}} + Z_L)} \tag{1}$$

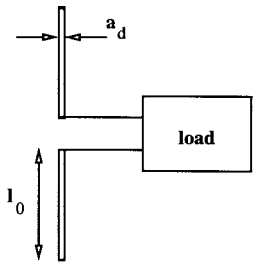

Fig. 1. Basic description of the electrically small loaded dipole antenna.

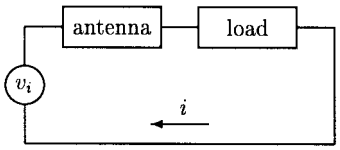

Fig. 2. Thevenin's equivalent circuit for an electric molecule.

where K_e is a constant which depends on the dimensions of the antenna and polarization coupling factors describing the relative orientation of the electric field components and the antenna. For the electrically small dipole antenna under consideration here, the input impedance is given by

$$Z_{\text{in}} = \frac{1}{-j\omega C_d} \tag{2}$$

where the constant $C_d = \pi\epsilon_0 l_0/\ln(4.0l_0/a_d)$ is the equivalent capacitance of the dipole antenna.

We also have obtained the corresponding time-domain behavior of these molecules. We have demonstrated [4]–[7], [18] that with single antenna molecules constructed from passive linear loads, one can obtain composite artificial materials whose electromagnetic response is described by traditional polarization models such as the Debye and Lorentz forms; their generalizations, e.g., the time-derivative Debye material (TD-DM), the time-derivative Lorentz material (TD-LM), the two time-derivative Lorentz material (2TD-LM), etc., to include more inclusive polarization behaviors; and even bianisotropic materials when multiple antenna molecules are considered [8].

Because it is based upon an indirect frequency-domain analysis, our previous approach is no longer effective if the loads are nonlinear. We now need to derive directly in the time domain the expressions for the currents at the terminals of the antennas and then determine the electromagnetic field radiated by those currents. We have shown [18] that the computation of the currents is now possible by solving a set of nonlinear ordinary differential equations describing the behavior of the total circuit, including the antenna and the load. In the case of the dipole antenna and its load, this modelization is obtained by representing the electric molecule by an equivalent Thevenin's circuit as shown in Fig. 2.

For the dipole antenna the current at its terminals i is related to the local electric field $\vec{E}$ at the antenna through the relations

$$\epsilon_0 \frac{\partial}{\partial t}\vec{E} = -\nabla \times \vec{H} - \frac{\partial}{\partial t}\vec{P} \tag{3}$$

$$\frac{\partial}{\partial t}\vec{P} = -\frac{l_0}{V} i\hat{n} \tag{4}$$

where $\vec{P}$ is the effective polarization of the dipole and $\hat{n}$ is the unit vector which represents its orientation. The constant V represents the effective volume associated with each molecule. We have taken the volume of the molecules to be a cubical volume surrounding each of them. To allow us to consider the composite material in a Maxwell–Garnett sense [19], [20], the volume was specified for the cases discussed below, unless specified otherwise, to be 318 times as large as the cylindrical volume of the antenna, i.e.,

$$\begin{aligned} V &= 5.0 l_0^3 \\ &= \left[\frac{5.0}{2.0\pi}\left(\frac{2.0 l_0}{a_d}\right)^2\right] \times \left[\pi\left(\frac{a_d}{2}\right)^2 (2l_0)\right] \\ &= 318.31 \times \left[\pi\left(\frac{a_d}{2}\right)^2 (2l_0)\right] \end{aligned} \tag{5}$$

which gives a 0.314% volume fill-factor for the material. Note that the source voltage for the circuit is given by the open circuit voltage of the receiving antenna with no load

$$v_i = -l_0 \vec{E} \cdot \hat{n}. \tag{6}$$

In a similar fashion, we can develop magnetic molecules from electrically small loop antennas and their loads. Unfortunately, as discussed in [18], nonlinear circuit devices available today are voltage-driven devices. For instance, there is no dual analog to a diode which is current driven. As a consequence, the magnetic molecules (which are current based) have very weak responses when loaded with those voltage-based devices. Thus, these nonlinear magnetic molecules are not pursued in this paper.

As with the linear passive loads, the specification of the passive and active nonlinear loads for the electric and magnetic molecules will determine the response of the resulting composite materials. The modeling of the circuit behavior can be accomplished readily with several numerical methods or the SPICE circuit simulation package [9]–[17]. The modeling of the interactions of an electromagnetic field with the composite material can be accomplished with augmentations of a FDTD simulator to include the additional time-domain ordinary differential equations that model the circuit voltages and currents [18].

The simplest nonlinear circuits use diodes in the loads. We have reported results for diode clamping and diode bridge molecules in an earlier work [18]. As an example of a passive nonlinear load, consider the two-diode circuit shown in Fig. 3. The capacitor represents the dipole antenna and has the capacitance C_d. The diodes are arranged in parallel with opposite positive orientation so that they are on for opposite polarities of the driving signal; hence, the circuit loads which produce the output signal are different for different signal polarities. If one imagines the diodes as interruptors, one can expect that this molecule will alternate its response between the molecules dictated by the local load impedances Z_1 and Z_2. As observed in the diode-based molecules studied in [18], the diodes will generate harmonics of the incident driving signal.

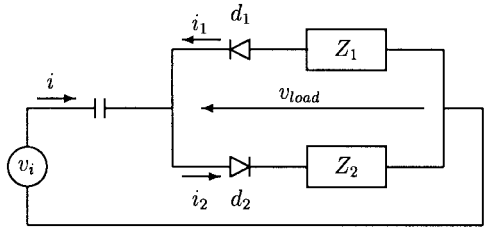

Fig. 3. Electric molecule nonlinear load circuit consisting of two diodes in parallel with opposite polarity and local impedances.

The response of this two-diode molecule is analyzed by considering the voltage and current equations for the circuit

$$v_i = v_c + v_{load} \tag{7}$$

$$v_{load} = -v_1 - v_{z1} = v_2 + v_{z2} \tag{8}$$

$$i_2 = i + i_1 \tag{9}$$

where the voltages across the diodes and the loads are labeled, respectively, as v_j and v_{zj} for $j = 1, 2$, and the voltage-current relations for the diodes and the capacitor

$$i_1 = I_s(e^{\alpha v_1} - 1) \tag{10}$$

$$i_2 = I_s(e^{\alpha v_2} - 1) \tag{11}$$

$$\frac{dv_c}{dt} = \frac{i}{C_d}. \tag{12}$$

If one considers the impedances Z_1 and Z_2 to be linear, the following time domain relationships between the voltages and the currents can be realized:

$$\sum_k p_k \frac{d^k v_{z1}}{dt^k} = \sum_j q_j \frac{d^j i_1}{dt^j} \qquad \text{load } Z_1 \tag{13}$$

$$\sum_k p'_k \frac{d^k v_{z2}}{dt^k} = \sum_j q'_j \frac{d^j i_2}{dt^j} \qquad \text{load } Z_2. \tag{14}$$

Several cases are possible.

- *Diode 1 Open, Diode 2 Closed:* The current $i_2 = -I_s$ so that $i = -i_1 - I_s$ and one obtains

$$\begin{aligned} \frac{dv_i}{dt} &= \frac{i}{C_d} - \frac{dv_1}{dt} - \frac{dv_{z1}}{dt} \\ &= \frac{i}{C_d} - \frac{1}{\alpha(i_1 + I_s)} \frac{di_1}{dt} - \frac{dv_{z1}}{dt} \end{aligned} \tag{15}$$

  thus

$$\frac{dv_i}{dt} = \frac{i}{C_d} - \frac{1}{\alpha i} \frac{di}{dt} - \frac{dv_{z1}}{dt}. \tag{16}$$

- *Diode 1 Closed, Diode 2 Open:* The current $i_1 = I_s$ so that $i = i_2 + I_s$ and one obtains in the same manner

$$\frac{dv_i}{dt} = \frac{i}{C_d} + \frac{1}{\alpha i} \frac{di}{dt} + \frac{dv_{z2}}{dt}. \tag{17}$$

- *Diode 1 and Diode 2 Closed:* The current $i_1 = i_2 = -I_s$ so that $i = 0$.

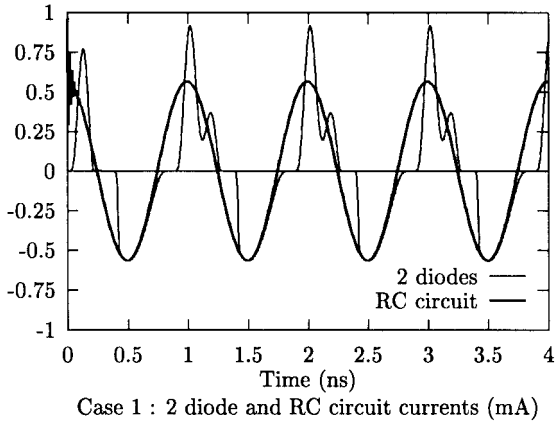

(a)

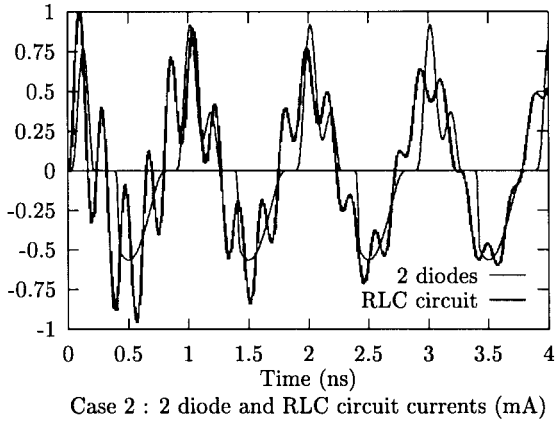

(b)

Fig. 4. Currents on an electric molecule whose nonlinear load circuit consists of two diodes in parallel with opposite polarity and connected locally to an R and a series RL segment. (a) Current time history on the electric molecule compared to the corresponding RC circuit. (b) Current time history on the electric molecule compared to the corresponding RLC circuit.

The first case is realized if one finds $i_1 > -I_s$; the second if $i_2 > -I_s$. The third case is obtained if $i_1 < -I_s$ and $i_2 < -I_s$.

To illustrate the effect of such two-diode molecules, consider the circuit in which Z_1 is simply a resistor R and Z_2 is a resistor R and an inductor L in series. From our linear materials analyzes this gives a Debye material model in the Z_1 path and a Lorentz model in the Z_2 path [5]. If the source is taken to be the sinusoidal driving signal

$$v_i = V_m \sin \omega t \tag{18}$$

with a driving frequency of 1.0 GHz, and the circuit consists of a resistor in the inductor arm with $R_1 = 10\ \Omega$, an inductor $L = 10.0$ nH, the capacitance $C = 9.0 \times 10^{-14} F = 0.09$ pF, and a resistor in the other arm with $R_1 = 10\ \Omega$, the driving point current on the antenna of this molecule is shown in Fig. 4(a) and (b). The currents generated on the corresponding RC- and RLC-only circuits are provided for comparison, respectively, in Fig. 4(a) and (b). These comparison results were obtained by solving the associated RC circuit equation

$$\frac{di}{dt} + \frac{i}{RC} = \frac{1}{R}\frac{dv_i}{dt} \tag{19}$$

which gives

$$i = \frac{V_m C_d \omega}{1 + (RC_d\omega)^2}\left(RC_d\omega \sin \omega t - \cos \omega t\right) \tag{20}$$

and the associated RLC circuit equation

$$\frac{d^2 i}{dt^2} + \frac{R}{L}\frac{di}{dt} + \frac{i}{LC_d} = \frac{1}{L}\frac{dv_i}{dt} \tag{21}$$

which gives the observed complex solution consisting of products of sinusoids at the angular frequencies ω and $\sqrt{1/LC_d - (R/2L)^2}$ and an attenuation factor $\exp(-Rt/L)$. One recognizes that the total current alternates between each of these components, closely recovering the negative half-cycle in the RC path and having a complicated oscillation resulting from the positive portion of the RLC path. The driving frequency is seen to underlie the overall response for either half-cycle. However, the diodes act as resets on each half-cycle so the attenuation factor of the RLC arm is experienced only during each positive half of the cycle and the RC decay of the RC arm on the negative half-cycle.

From these results one could thus use this two-diode molecule to encode different information on each half-cycle of the output signal, hence, it could be used in multiplexing the output signals. Another possibility is to have the loads selected to produce reflection coefficients of opposite sign on each half-cycle. This would lead to an null average, hence, the material would look as if it were a matched material on average. A third molecule and reflection coefficient may be necessary to complete the null average if the time lag between the responses from the Z_1 and Z_2 arms is large enough to make the averaging slightly different from zero. One also could consider using this two-diode type of molecule as a two-bit curve shaper where the current in each half-cycle takes a form specified by the linear circuit. However, we will not pursue this molecule any further.

The scattering response of the corresponding two-diode molecule material is obtained in a straightforward manner. As with any passive or active molecule, the circuit equations governing the voltage and current response of the load are solved simultaneously with Maxwell's equations (3) and (4). A single molecule is associated with each cell in the material; thus, it is assumed that each molecule is much smaller than the cell size and can be treated as a lumped element. The resulting augmented FDTD simulator treats the field seen by each molecule as the local field at that molecule. As the local field interacts with a molecule, the resulting field scattered by that molecule propagates to all neighboring mesh points, hence, molecules through the FDTD scheme in a retarded Green's function sense. Thus, all mutual interactions between the fields and each molecule are taken into account in any augmented FDTD simulation. The response of the material predicted by the FDTD simulator, for instance, in the two-diode molecule material, closely mimics that of the loaded antenna treated as a circuit element. Deviations, of course, occur because of the mutual interactions between all of the molecules and the fields in the material. The magnitude of these deviations depends intimately on the strength of those interactions.

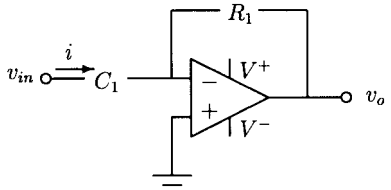

Fig. 5. Operational amplifier differentiator (OAD) circuit.

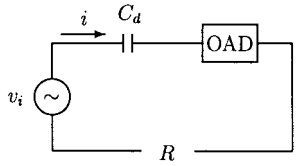

Fig. 6. Equivalent Thevenin's circuit for the OAD connected to a dipole antenna.

III. Op Amp Differentiating Molecules

By introducing operational amplifiers into the loads, active molecules can be designed to have a number of interesting signal transformation properties which are then transferred directly into the scattering response of the corresponding artificial material. Note that we have assumed ideal op-amps in this study to simplify the analysis. More realistic op-amp, hence, molecular behaviors could be readily incorporated into the simulations through lookup tables if desired. This is one of the strengths of the augmented FDTD simulator.

Because the op amp is a voltage driven device, it leads naturally to nonlinear electric molecules, hence, to dielectric composite materials. These basic nonlinear molecules and their FDTD simulations are treated in this section. More complicated loads are dealt with in the following sections. Throughout, we assume an x-polarized electromagnetic plane wave is incident on the molecules and that they are aligned along the positive x-axis.

A. Differentiating Circuit

We introduce into the load the well known differentiating circuit shown in Fig. 5. This operational amplifier differentiator (OAD) circuit leads to the following relation between the input voltage $v_{\rm in}$ and the output voltage v_o

$$v_o = -R_1 C_1 \frac{dv_{\rm in}}{dt}. \tag{22}$$

When it is connected to a dipole antenna and a load resistor R (plus a small resistor r to prevent undesired noise), we obtain the equivalent Thevenin's circuit shown in Fig. 6. This molecule is thus described by the following:

$$v_o = Ri = -R_1 C_1 \frac{dv_{\rm in}}{dt} \tag{23}$$

$$v_{\rm in} = v_i - v_C - ri = -l_0 E - v_C - ri. \tag{24}$$

Then, plugging (24) into (23) and using (3) and (4), we find the following differential equation for the current at the terminals of the dipole antenna:

$$\frac{di}{dt} - \left(\frac{R}{R_1 C_1} - \frac{1}{C_d} - \frac{l_0^2}{\epsilon_0 V}\right)\frac{i}{r} = \frac{l_0}{r\epsilon_0}\frac{\partial H_y}{\partial z}. \tag{25}$$

This current describes the response of the molecule to the local electromagnetic field. In the case where the coefficient

$$\frac{1}{\tau} = \frac{1}{r}\left(\frac{1}{C_d} + \frac{l_0^2}{\epsilon_0 V} - \frac{R}{R_1 C_1}\right) \tag{26}$$

is positive, this equation can be solved easily with the FDTD schemes introduced in [18]. We note that one must check for the saturation of each op amp at each time step when solving (25).

B. Integrating Circuit

Swapping C_1 and R_1 in the circuit of Fig. 5 leads to the op amp integrating (OAI) circuit, characterized by the relation

$$v_{\rm in} = -R_1 C_1 \frac{dv_o}{dt}. \tag{27}$$

A simple analysis of the equivalent Thevenin's circuit of the OAI dielectric molecule shows that a regular increase of the current leads very quickly to saturation of the op amp, hence, to poor performance of this molecule. Therefore, we did not pursue this circuit and associated molecule any further.

C. FDTD Results

The computation of the x-polarized EM field scattered by a slab of the dielectric OAD molecules was made by implementing (25) into our augmented one-dimensional (1-D) FDTD Maxwell solver. We used a leap frog scheme where:

- the electric field is labeled $E_k^n = E_x(n\Delta t, k\Delta z)$;
- the magnetic field is labeled $H_{k+1/2}^{n+1/2} = H_y((n+1/2)\Delta t, (k+1/2)\Delta z)$;
- the current is labeled as $i_k^{n+1/2} = i((n+1/2)\Delta t, k\Delta z)$.

Thus, the electric and magnetic field points are staggered in the usual FDTD sense in space and time and the dipole currents are collocated spatially with the electric field points and temporally with the magnetic field points. Discretizing (3), (4), and (25) leads to the following set of equations that must be solved for the space–time evolution of the electromagnetic field:

$$H_{k+1/2}^{n+1/2} = H_{k+1/2}^{n-1/2} - \frac{\Delta t}{\mu_0 \Delta z}\left(E_{k+1}^n - E_k^n\right) \tag{28}$$

$$i_k^{n+1/2} = i_k^{n-1/2}\exp(-\Delta t/\tau) + \frac{l_0 \Delta t}{2r\epsilon_0 \Delta z} \times \exp(-\Delta t/2\tau) \tag{29}$$

$$\times \left(H_{k+1/2}^{n+1/2} + H_{k+1/2}^{n-1/2} - H_{k-1/2}^{n+1/2} - H_{k-1/2}^{n-1/2}\right) \tag{30}$$

$$E_k^{n+1} = E_k^n + \frac{l_0 \Delta t}{V} i_k^{n+1/2} - \frac{\Delta t}{\epsilon_0 \Delta z} \times \left(H_{k+1/2}^{n+1/2} - H_{k-1/2}^{n+1/2}\right). \tag{31}$$

The incident electric field was launched toward the artificial material region from a total field/scattered field interface located in a free-space region. The incident electric field was assumed to have the form

$$E^i = \left[1 - \left(\frac{t - T/2}{T/2}\right)^2\right]^4 \sin(\omega_0 t) \tag{32}$$

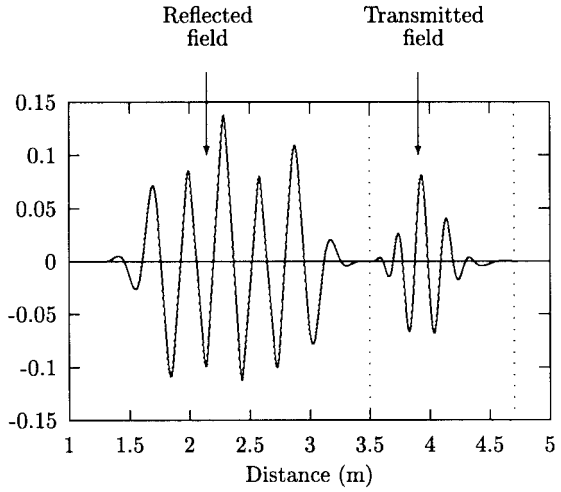

Fig. 7. The electric field E_x (V/m) as a function of the distance (m) in the simulation region.

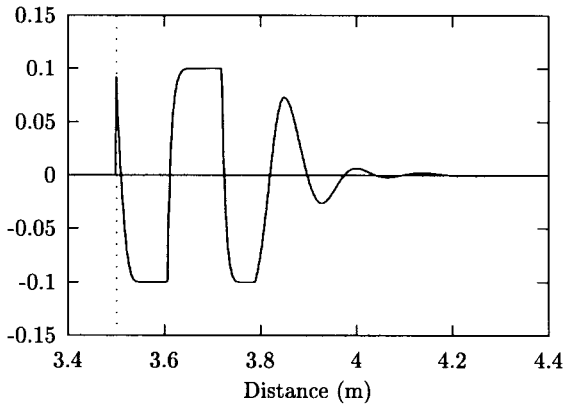

Fig. 8. The current (mA) at the terminals of the antennas inside the medium at one simulation time step as a function of the distance (m) in the simulation region.

which is an unit amplitude pulse modulated by a sinusoidal wave with a total time record length of T s. The frequency of the incident field is $f_0 = 1.0$ GHz, the pulse length is $T = 8.0/f_0 = 8.0$ ns or $cT = 2.4$ m, the half-length of the dipole is $l_0 = 3.0$ cm, the diameter of the dipole is $a_d = l_0/10 = 3.0$ mm. The volume associated with the molecule was defined by (5).

The circuit resistances were $R = 100\ \Omega$ and $r = 20\ \Omega$; the resistance and capacitance of the OAD were, respectively, $R_1 = 30\ \mathrm{k}\Omega$ and $C_1 = 10^{-15}$ F $= 0.001$ pF. A snapshot in time of the electric field (in V/m) reflected from and transmitted into the slab is given in Fig. 7. The dash vertical lines represent the boundaries of the OAD-molecule medium. We can see that both the amplitude of the reflected and the transmitted fields are reduced in magnitude, implying absorption in the medium. The shape is also different from that of the incident field. Fourier analysis of the reflected field yields a spectrum which contains the input angular frequency ω_0, its low order odd harmonics $(2n+1)\omega_0$, and even the half subharmonic at the frequency $\omega_0/2$. Thus, the OAD molecule medium has produced signals with a rich frequency content from a narrow bandwidth incident waveform. This pecular subharmonic frequency behavior appears to be caused by the saturation of the op amps. Fig. 8 shows a snapshot of the current at the terminals of each antenna after the incident field has entered the medium. One clearly can see that at any one time the current across several op amps molecules have reached their saturation values

IV. Op Amp Loaded Linear Molecules

The op-amp-based circuits can also be used to tailor the electromagnetic characteristics of the "linear" synthetic materials. We will illustrate these possibilities with two examples: the negative impedance convertor and the phase shifter.

A. Negative Impedance Converter

The negative impedance converter (NIC) changes the sign of a given load. It is the op-amp-based circuit shown in Fig. 9.

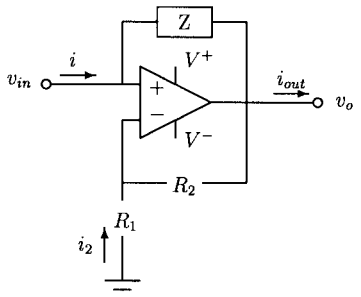

Fig. 9. Negative impedance converter (NIC) circuit.

If we suppose that the op amp is in its linear region, the input impedance is given by the expression

$$Z_{eq} = \frac{v_{\mathrm{in}}}{i} = -Z\,\frac{R_1}{R_2}. \tag{33}$$

If we assume that the resistors $R_1 = R_2$, then this NIC circuit's impedance is equivalent to the opposite of the load impedance Z. This circuit can be used to cancel the input impedance of the antenna in a linearly loaded molecule by having $Z_{eq} = -Z_{\mathrm{in}}$. Note that because the op amp is used as a *linear* complex component, we could also use it with a loop antenna to obtain dual materials.

We consider the equivalent circuits for the electric molecules shown in Fig. 10. The dipole's load is composed of a given impedance Z_l in series with the NIC circuit loaded with the equivalent capacitance of the antenna. We obtain the electric susceptibility with (1) by assuming $Z_L = Z_l - Z_{\mathrm{in}}$. This leads to the expression

$$\chi_e = \frac{K_e}{-j\omega Z_l}. \tag{34}$$

For example, in the case of a resistive load, the corresponding relative permittivity becomes

$$\epsilon_r = 1 + j\,\frac{K_e}{R\omega}. \tag{35}$$

The electromagnetic behavior of this dielectric NIC material is thus governed by the following differential equation:

$$\frac{\partial E_x}{\partial t} + \frac{K_e}{R\epsilon_0}\,E_x = -\frac{1}{\epsilon_0}\,\frac{\partial H_y}{\partial z}. \tag{36}$$

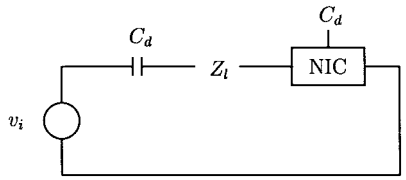

Fig. 10. NIC circuits: Equivalent Thevenin's circuit for the dielectric molecule.

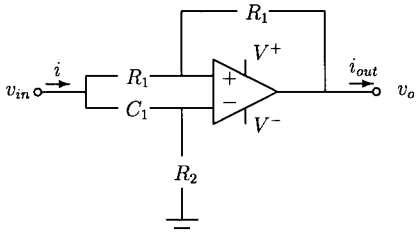

Fig. 11. Phase shifter circuit.

This artificial material acts as a lossy dielectric whose conductivity, hence, loss tangent is adjustable by the magnitude of the resistor. However, unlike a conductive material, which has high loss at low frequencies and low loss at high frequencies, this artificial dielectric could be designed to have small or large losses at either low or high frequencies.

B. Phase Shifter Circuit

The circuit shown in Fig. 11 is a phase shifter (PS) which is characterized by the voltage magnitude and phase responses

$$\left|\frac{v_o}{v_{\text{in}}}\right| = \left|\frac{-jR_2C_1\omega - 1}{-jR_2C_1\omega + 1}\right| = 1 \tag{37}$$

$$\begin{aligned}\phi &= \arg(v_o/v_{\text{in}}) \\ &= 180 - 2\arctan(R_2C_1\omega).\end{aligned} \tag{38}$$

This means the output and input voltages have the same amplitude but a different phase.

If we insert this device into a dielectric molecule, we obtain the equivalent circuit shown in Fig. 12 which leads to the voltage expression

$$v_i = v_C + (v_{\text{in}} - v_o) + Zi_{\text{out}} = v_C + Z_{eq}i \tag{39}$$

where the output voltage

$$v_o = v_{\text{in}}e^{j\phi}. \tag{40}$$

The equivalent total impedance of the molecule load ($Z+\text{PS}$) is

$$Z_{eq} = \frac{Z}{1 - jR_1C_1\omega}\, e^{-j\phi} \tag{41}$$

and can be plugged into (1) to obtain the equivalent susceptibility of this molecule.

Fig. 13 shows the real and imaginary parts of the relative permittivity ϵ_r for an artificial Lorentz material (series RLC load [4]) and a PS-enhanced artificial Lorentz material (Z_{eq} is in series with the RLC load). We can see from Fig. 13 that the resonant characteristic of the Lorentz material is lost when the PS is present. The relative permittivity now has a more complex frequency behavior leading to large losses over a large bandwidth.

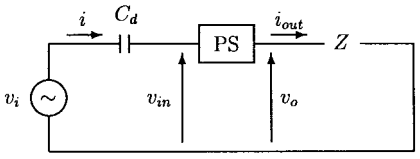

Fig. 12. Phase-shifter circuit in an electric molecule.

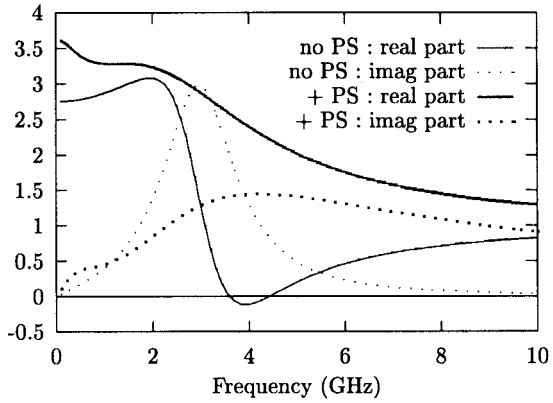

Fig. 13. Phase shifter circuit is inserted into a dielectric Lorentz model. Comparison of the relative permittivity ϵ_r with and without the PS circuit enhancement.

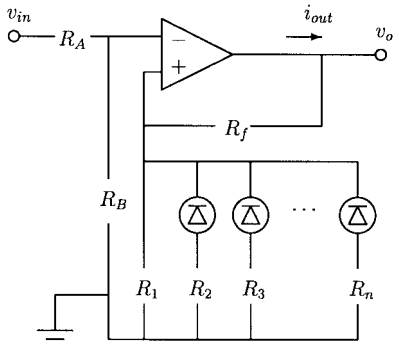

Fig. 14. Curve-shaper circuit. Approximation by n linear segments.

V. Curve Shapers: Toward Smart Molecules

The curve shaper (CS) circuit is designed to approximate a given function with several linear segments. This circuit combines an op amp with a set of Zener diodes. An n-segment CS circuit is shown in Fig. 14.

The op amp is used across n different voltage regions. In each region the slope of the segment is the CS gain. These regions are bounded by the avalanche voltages V_i of the Zener diodes. For instance, if $V_i < v_o < V_{i+1}$, the gain of the ith region is

$$\frac{v_o}{v_{\text{in}}} = A_i = \frac{R_B}{R_A + R_B}\,\frac{R_{||} + R_f}{R_{||}} \tag{42}$$

and the output current is $i_{\text{out}} = -R_B i/R_{||}$, where $R_{||}$ is the total parallel resistance obtained from the individual resistors R_1 to R_i.

Thus, if this CS circuit is used to approximate the function $v_o = f(v_{\rm in})$ and we insert it into the load of a dielectric Debye molecule (in series with the resistor R), we obtain the input voltage $v_{\rm in} = v_i - v_c$ and the output voltage

$$v_o = Ri_{\rm out} = -\frac{R}{R_f}\left((R_A + R_B)f'(v_{\rm in}) - R_B\right)i \tag{43}$$

where $A(v_{\rm in}) = f'(v_{\rm in})$. This result leads to the following differential equation for the voltage across the dipole antenna

$$\frac{dv_c}{dt} = \frac{R_f}{RC_d}\,\frac{f(v_i - v_c)}{R_B - (R_A + R_B)f'(v_i - v_c)}. \tag{44}$$

The implementation of this CS circuit in the FDTD code is accomplished by solving a system of two differential equations composed of (44) and the electric field update equation

$$\epsilon_0\,\frac{\partial E_x}{\partial t} = -\frac{\partial H_y}{\partial z} + \frac{l_0 C_d}{V}\,\frac{dv_c}{dt}. \tag{45}$$

This equation is discretized by finite differences to obtain

$$E_k^{n+1} = E_k^n - \frac{\Delta t}{\epsilon_0 \Delta z}\left[H_{k+1/2}^{n+1/2} - H_{k-1/2}^{n+1/2}\right] + \frac{l_0 C_d}{\epsilon_0 V}\left(v_c^{n+1} - v_c^n\right) \tag{46}$$

which can be used to compute v_i using (6). This expression for v_i is inserted in (44); the resulting equation can then be solved for v_c^{n+1} with a simple Runge Kutta solver [21]. Thus, to achieve a FDTD implementation of the CS molecule we need to use a combined finite difference-differential equation approach.

To test the behavior of a CS molecule, we used the CS circuit to approximate the function $v_o = f(v_{\rm in}) = \alpha v_{\rm in}^3$ with five and three segments as shown in Fig. 15. Because v_i is proportional to E_x, this choice of f should make the resulting composite material act as a Kerr medium; i.e., it should produce odd-harmonics of the input signal. In the five segment case both the positive and negative portions of the voltage are recovered; in the three segment case only the positive portion is modeled. The CS circuit required the resistors $R_A = 100.0\ \Omega$, $R_B = 10.0\ \Omega$, and $R_f = 200\ \Omega$, and the constant $\alpha = 30.0V^{-2}$. The values of the curve-fit points required in (44) were calculated directly from the function f. The CS molecule was composed of a dipole antenna with half-length $l_0 = 1.0$ cm and diameter $a_d = l_0/10 = 1.0$ mm connected to a resistor $R = 10.0\ \Omega$ and it was assumed to have an effective volume $V = 5.0l_0^3$.

The electric fields reflected and transmitted from the CS material with five and three segments are given, respectively, in Figs. 16 and 17. The differences in the approximations result in obvious differences in the reflected fields. In the five-segment case in Fig. 16, one can find only the odd low-order harmonics of the input frequency in the spectrum of the reflected field which corresponds to the expected Kerr medium behavior. In the three-segment case in Fig. 17, every harmonic is present because the signal is now rectified. The reflected field is rectified in the three-segment case because the response in the negative portion of the input voltage is approximately zero.

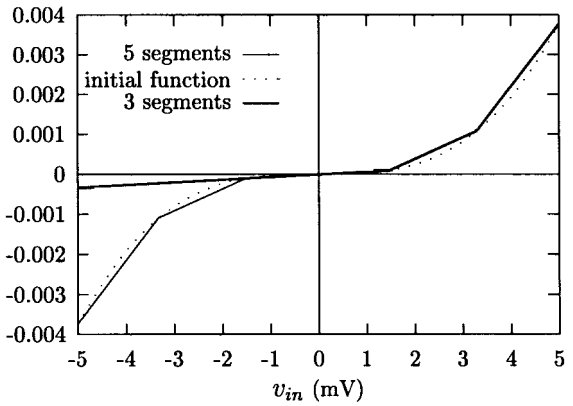

Fig. 15. The output voltage function $v_o = f(v_{\rm in})$ (mV) and its five- and three-segment approximations as a function of the input voltage (mV).

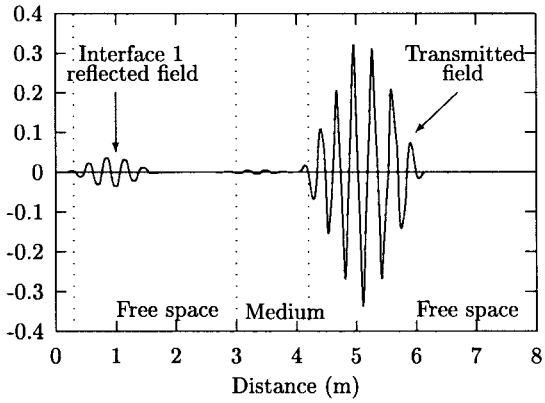

Fig. 16. The electric fields (V/m) reflected from and transmitted through a slab of CS material composed of five-segment curve fitting molecules versus the distance in the simulation region (m).

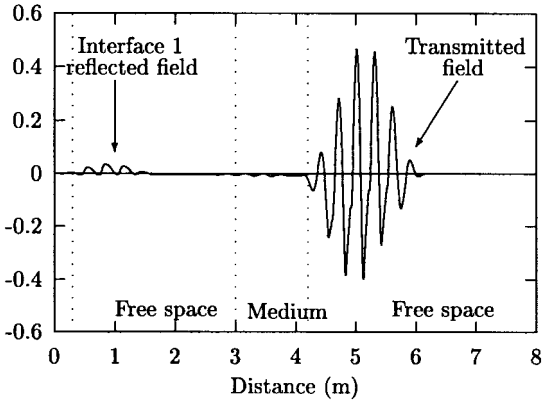

Fig. 17. The electric fields (V/m) reflected from and transmitted through a slab of CS material composed of three-segment curve fitting molecules versus the distance in the simulation region (m).

The CS circuit can be used to approximate any kind of function f, even with negative slopes provided we can use negative resistance devices. The latter are possible with the op amp circuits. It would, therefore, be possible to design the CS circuit to obtain any kind of reflected field which has in its spectrum the harmonics of the input frequency. For instance, if one wanted a passive target recognition signal, one could design a CS molecule that would respond with a

specified waveform to a predetermined input signal. A patch of this artificial material on a surface could then be interrogated (if desired) to determine, for example, a friend-or-foe status. Furthermore, knowing that the R_i, $i = 1, \cdots, n$ resistors in the CS circuit are the knobs that can actually modify the function, it would be possible to design a microwave smart material that could be adjusted to have a specified response to a given incident field, just by replacing those resistors by some commanded set of variable resistors. Feedback from a sensor that captures information about the incident field could be used to adjust the resistor values in real time, thus, actively tuning the output of the material. Such a material could act as a "smart skin" coating on any scatterer.

VI. Conclusions

We have shown in previous papers that artificial materials composed of linearly loaded molecules (i.e., electrically small antennas connected to linear electronic circuits) could lead to some well-known dispersive, lossy materials such as the Debye and the Lorentz models and to their generalizations, which include time derivatives of the incident fields as their driving signals. The possibility of designing matched materials, i.e., dielectric and magnetic materials having $\epsilon_r = \mu_r$, has been discussed as well as the potential for designing bianisotropic and tensor materials with specified electromagnetic responses.

In the present work, these linear molecules have been extended to active loads based on multiple diode and op-amp circuits. We have shown that the resulting nonlinear molecules can include electrically small antennas loaded with OAD's, NIC's, and PS's. The OAD's lead to materials which transform single-frequency signals into time-domain waveforms containing the fundamental and higher order harmonics as well as subharmonics. The subharmonics appear because of the saturation effects associated with the op amp. The NIC's can be used to compensate for the antenna impedance so that its response is not limited by that impedance. Electric molecules were designed that lead to an artificial material in which the losses at any frequency can be adjusted to any desired value. The PS circuits led to materials which had enhanced bandwidths to their responses by eliminating characteristic singular behaviors.

We further introduced molecules that have curve shaping abilities. A CS molecule can be designed to replicate approximately any functional behavior. The response of a composite material formed with these curve shaping molecules can be used to generate desired signals from single-frequency inputs. The CS molecules provide a means to design a composite material that could respond in real time to an interrogative signal in a predefined manner. This material could be used as a coating on aircraft, ships, or cars. Such "smart skins" could be used for identification purposes during manufacturing as well as in their intended environments. Many other possibilities have not been addressed, which include op-amp circuits that could involve oscillators, frequency dividers, or frequency multipliers. The ability to simulate the integration of such nonlinear circuits into a molecule's load with an augmented FDTD simulator has been demonstrated. The final determination of which nonlinear circuit should be investigated now depends on the one most appropriate for the intended application.

As with any artificial molecule that we have studied, issues about the availability of circuit components at the desired sizes and frequencies arise. The op amp circuits further stress these considerations because there is now a need to provide some external voltage sources (V^+ and V^-) to the op amps. Nonetheless, we have found integrated circuit packages with sizes corresponding to those needed in the low microwave region. Higher frequencies may be attainable in the near future. The inverse problem of defining which curve-shaping circuit will produce a specific waveform from the composite material has not been dealt with here. We simply selected a simple functional form for the CS molecule and demonstrated that it produces a particular response. Many other functional forms are possible with such CS circuits and they need to be investigated further. The possibility of designing artificial materials with specified active responses warrants further developments in this area.

References

[1] I. V. Lindell, A. H. Sihvola, S. A. Tretyakov, and A. J. Vitanen, *Electromagnetic Waves in Chiral and Bi-Isotropic Media.* Boston, MA: Artech House, 1994, pp. 8–14.

[2] F. Mariotte, S. A. Tretyakov, and B. Sauviac, "Isotropic chiral composite modeling: Comparison between analytical, numerical, and experimental results," *Microwave Opt. Technol. Lett.*, vol. 7, no. 18, pp. 861–864, 1994.

[3] F. Mariotte and J.-P. Parneix, Eds., Proc. Chiral'94 Workshop, 3rd Int. Workshop Chiral, Bi-Isotropic, Bi-Anisotropic Media, Perigueux, France, May 1994.

[4] R. W. Ziolkowski and F. Auzanneau, "The design of maxwellian smart skins," in *Proc. 13th ACES Symp.*, Monterey, CA, Mar. 1997, pp. 98–103.

[5] ———, "Passive artificial molecule realizations of dielectric materials," *J. Appl. Phys.*, vol. 82, no. 7, pp. 3195–3198, Oct. 1997.

[6] ———, "Artificial molecule realizations of a magnetic wall," *J. Appl. Phys.*, vol. 82, no. 7, pp. 3192–3194, Oct. 1997.

[7] F. Auzanneau and R. W. Ziolkowski, "Étude théorique de matériaux bianisotropes synthétiques contrŏlables," *Journal de Physique III*, vol. 7, pp. 2405–2418, Dec. 1997.

[8] ———, "Theoretical study of synthetic bianisotropic materials," *J. Electromagn. Waves Applicat.*, vol. 12, no. 3, pp. 353–370, Dec. 1997.

[9] B. Toland, J. Lin, B. Houshmand, and T. Itoh, "FDTD analysis of an active antenna," *IEEE Microwave Guided Wave Lett.*, vol. 3, pp. 423–425, Nov. 1993.

[10] B. Toland and T. Itoh, "Modeling of nonlinear active regions with the FDTD method," *IEEE Microwave Guided Wave Lett.*, vol. 3, pp. 333–335, Sept. 1993.

[11] C.-N. Kuo, V. A. Thomas, S. T. Chew, B. Houshmand, and T. Itoh, "Small signal analysis of active circuits using FDTD algorithm," *IEEE Microwave Guided Wave Lett.*, vol. 5, pp. 216–218, July 1995.

[12] C.-N. R.-B. Wu, Kuo, B. Houshmand, and T. Itoh, "Modeling of microwave active devices using the FDTD analysis based on the voltage-source approach," *IEEE Microwave Guided Wave Lett.*, vol. 6, pp. 199–201, May 1996.

[13] C.-N. Kuo, B. Houshmand, and T. Itoh, "Full-wave analysis of packaged microwave circuits with active and nonlinear devices: An FDTD approach," *IEEE Trans. Microwave Theory Tech.*, vol. 45, pp. 819–826, May 1997.

[14] M. Piket-May, A. Taflove, and J. Baron, "FD-TD modeling of digital signal propagation in 3-D circuits with passive and active loads," *IEEE Trans. Microwave Theory Tech.*, vol. 42, pp. 1514–1523, Aug. 1994.

[15] V. A. Thomas, M. E. Jones, M. Piket-May, A. Taflove, and E. Harrigan, "The use of SPICE lumped circuits as subgrid models for FDTD analysis," *IEEE Microwave Guided Wave Lett.*, vol. 4, pp. 141–143, May 1994.

[16] M. A. Alsunaidi, S. M. Sohel Imtiaz, and S. M. El-Ghazaly, "Electromagnetic wave effects on microwave transistors using a full-wave

time-domain model," *IEEE Trans. Microwave Theory Tech.,* vol. 44, pp. 799–808, June 1996.
[17] W. Sui, D. A. Christensen, and C. H. Durney, "Extending the two-dimensional FD-TD method to hybrid electromagnetic systems with active and passive lumped elements," *IEEE Trans. Microwave Theory Tech.,* vol. 40, pp. 724–730, Apr. 1992.
[18] F. Auzanneau and R. W. Ziolkowski, "Microwave signal rectification using artificial composite materials composed of diode-loaded, electrically small dipole antennas," *IEEE Trans. Microwave Theory Tech.,* vol. 46, pp. 1628–1637, Nov. 1998.
[19] I. V. Lindell, A. H. Sihvola, S. A. Tretyakov, and A. J. Vitanen, *Electromagnetic Waves in Chiral and Bi-Isotropic Media.* Boston, MA: Artech House, 1994, pp. 208–209.
[20] R. J. Gehr and R. W. Boyd, "Optical properties of nanostructured optical materials," *Chem. Material,* vol. 8, no. 8, pp. 1807–1819, 1996.
[21] R. F. Churchhouse, Ed., *Handbook of Applicable Mathematics, Vol. III: Numerical Methods.* New York: Wiley, 1981, pp. 321–325.

Fabrice Auzanneau received the Dipl. from the Ecole Nationale Superieure de l'Aeronautique et de l'Espace, Toulouse, France, in 1987.

He is an Engineer and has been working at the CEA CESTA Laboratory, Bordeaux, France, since 1988 on topics related to electromagnetism and stealth. He was a Visiting Scholar with the Department of Electrical and Computer Engineering, University of Arizona, Tucson, from 1996 to 1997.

Richard W. Ziolkowski (M'87–SM'91–F'94) received the Sc.B. degree in physics (*magna cum laude*) with honors from Brown University, Providence, RI, in 1974, and the the M.S. and Ph.D. degrees in physics from the University of Illinois at Urbana-Champaign, in 1975 and 1980, respectively.

He was a member of the Engineering Research Division at the Lawrence Livermore National Laboratory from 1981 to 1990 and served as the Leader of the Computational Electronics and Electromagnetics Thrust Area for the Engineering Directorate from 1984 to 1990. He joined the Department of Electrical and Computer Engineering, University of Arizona, Tucson, as an Associate Professor in 1990 and was promoted to Full Professor in 1996. His research interests include the application of new mathematical and numerical methods to linear and nonlinear problems dealing with the interaction of acoustic and electromagnetic waves with realistic materials and structures.

Dr. Ziolkowski is a member of several honorary and professional societies including Tau Beta Pi, APS, and OSA. He is a member of Commissions B (Fields and Waves) and D (Electronics and Photonics) of URSI (International Union of Radio Science). He was the United States URSI Commission B Secretary from 1993 to 1996 and is currently serving as the Chairperson of the Technical Activities Committee of Commission B. He was an Associate Editor for the IEEE TRANSACTIONS ON ANTENNAS AND PROPAGATION from 1993 to 1998. He served as the Vice Chairman of the 1989 IEEE/AP-S and URSI Symposium in San Jose, CA, and as the Technical Program Chair for the 1998 IEEE Conference on Electromagnetic Field Computation (CEFC'98) Conference in Tucson, AZ. He was awarded the Tau Beta Pi Professor of the Year Award in 1993 and the IEEE and Eta Kappa Nu Outstanding Teaching Award in 1993 and 1998.